

# Screening and Identification of Small Molecule Compounds Perturbing Mitosis Using Time-Dependent Cellular Response Profiles

Ning Ke,<sup>\*,†,‡</sup> Biao Xi,<sup>†,‡</sup> Peifang Ye,<sup>‡</sup> WanHong Xu,<sup>‡</sup> Min Zheng,<sup>‡,§</sup> Long Mao,<sup>†</sup> Meng-Jou Wu,<sup>†</sup> Jenny Zhu,<sup>†,‡</sup> Jieying Wu,<sup>‡</sup> Wenfu Zhang,<sup>†</sup> Jing Zhang,<sup>†</sup> Jeff Irelan,<sup>†</sup> Xiaobo Wang,<sup>†</sup> Xiao Xu,<sup>†,‡</sup> and Yama A. Abassi<sup>\*,†</sup>

Department of Cell Biology and Assay Development, ACEA Biosciences, San Diego, California 92121, Hangzhou High Throughput Drug Screening Center, ACEA Bio, Hangzhou, Zhejiang, P.R. China, and State Key Laboratory for Diagnosis and Treatment of Infectious Disease, First Affiliated Hospital, College of Medicine, Zhejiang University, Hangzhou, Zhejiang 310003, P.R. China

Cellular processes such as cell cycle progression, mitosis, apoptosis, and cell migration are characterized by well-defined events that are modulated as a function of time. Measuring these events in the context of time and its perturbation by small molecule compounds and RNAi can provide mechanistic information about cellular pathways being affected. We have used impedance-based time-dependent cell response profiling (TCRP) to measure and characterize cellular responses to antimitotic compounds or siRNAs. Our findings indicate that small molecule perturbation of mitosis leads to unique TCRP. We have further used this unique TCRP signature to screen 119 595 compound library and identified novel antimitotic compounds based on clustering analysis of the TCRPs. Importantly, 113 of the 117 hit compounds in the TCRP antimitotic cluster were confirmed as antimitotic based on independent assays, thus establishing the robust predictive nature of this profiling approach. In addition, potent and novel agents that induce mitotic arrest either by directly interfering with tubulin polymerization or by other mechanisms were identified. The TCRP approach allows for a practical and unbiased phenotypic profiling and screening tool for small molecule and RNAi perturbation of specific cellular pathways and time resolution of the TCRP approach can serve as a complement for other existing multidimensional profiling approaches.

One of the hallmarks of neoplastic transformation is the evasion of key regulatory mechanisms that safeguard the precise entry and transition of cells into the various phases of the cell cycle. For example, p53 which is involved in sensing the integrity of DNA during the S phase of the cell cycle is mutated in more than 50% of human cancers.<sup>1</sup> Due to the loss or perturbation of these crucial cell cycle regulatory factors, cancer cells continue to grow and proliferate unabated.<sup>2</sup> This unregulated growth and prolifera-

tion, while contributing to tumor mass and volume, also provides a window of opportunity for chemotherapeutic intervention. Hence, a common strategy for cancer chemotherapy has been to develop drugs that interrupt the cell cycle.<sup>2</sup> By far, compounds that interfere with DNA synthesis and mitosis machineries are among the most important components of the chemotherapeutic regimens.<sup>3,4</sup> While DNA damaging agents either alter the structure of DNA or hinder DNA synthesis leading to cell cycle specific or nonspecific cell death, antimitotic agents induce mitotic (M) phase arrest and eventual cell demise.<sup>5,6</sup>

The mitotic phase of the cell cycle is a well orchestrated set of molecular events that ultimately lead to the faithful separation of sister chromatids into two individual daughter cells.<sup>5,7</sup> Failure of cells to properly segregate their chromosomes results in mitotic arrest through activation of the M phase or spindle assembly checkpoint (SAC), culminating in cell death or aberrant exit from mitosis in the absence of cytokinesis.<sup>5,7–9</sup> Drugs such as Vinca alkaloids and taxanes target the microtubule cytoskeleton and induce mitotic arrest/apoptosis, and are currently in clinical use against a number of cancers including leukemias and lymphomas, lung, breast, and ovarian cancers.<sup>10</sup> It is believed that the specificity of tubulin targeting agents for cancer cells arise from their apparent affinity for spindle microtubules during mitosis. Because spindle microtubules are highly dynamic, they are more prone to tubulin targeting agents, especially at lower drug concentrations, compared to interphase microtubules which appear to be less dynamic. Due to the apparent dose-limiting toxicities associated with current antimitotic agents as well as acquisition of tumor cell resistance, considerable effort has been invested in identifying novel antimitotic agents with greater potency and specificity.<sup>5,7,8</sup>

We have previously described a novel functional cell-based assay system for profiling and identifying mechanism of action of

\* To whom correspondence should be addressed. E-mail: nke@aceabio.com (N. K.); yabassi@aceabio.com (Y. A.).

† Department of Cell Biology and Assay Development, ACEA Biosciences.

‡ Hangzhou High Throughput Drug Screening Center.

§ Zhejiang University.

(1) Levine, A. J. *Cell* **1997**, *88*, 323–331.

(2) Lapenna, S.; Giordano, A. *Nat. Rev. Drug Discov.* **2009**, *8*, 547–566.

(3) Chabner, B. A.; Roberts, T. G., Jr. *Nat. Rev. Cancer* **2005**, *5*, 65–72.

(4) DeVita, V. T., Jr.; Chu, E. *Cancer Res.* **2008**, *68*, 8643–8653.

(5) Schmidt, M.; Bastians, H. *Drug Resist. Update* **2007**, *10*, 162–181.

(6) Johnstone, R. W.; Ruefli, A. A.; Lowe, S. W. *Cell* **2002**, *108*, 153–164.

(7) Jackson, J. R.; Patrick, D. R.; Dar, M. M.; Huang, P. S. *Nat. Rev. Cancer* **2007**, *7*, 107–117.

(8) Gascoigne, K. E.; Taylor, S. S. *J. Cell Sci.* **2009**, *122*, 2579–2585.

(9) Weaver, B. A.; Cleveland, D. W. *Cancer Cell* **2005**, *8*, 7–12.

(10) Jordan, M. A.; Wilson, L. *Nat. Rev. Cancer* **2004**, *4*, 253–265.

small molecule compounds.<sup>11</sup> The strategy is based on continuous monitoring of cell substrate impedance in real-time which produces very specific time-dependent cellular response profiles (TCRP) upon treatment with biologically active compounds. TCRP can be predictive of mechanism of action, as compounds with similar biological activity often produce similar signature TCRP. In this study, we have extended these studies and focused on the signature TCRP mediated by antimitotic agents. We use a range of molecular and cell biological techniques to characterize and validate this unique pattern. Furthermore, we demonstrate the utility of this profiling approach by screening a 119 595 compound library and identifying novel compounds which interfere with the mitotic phase of the cell cycle. Some of these compounds appear to interfere with tubulin polymerization, while a subset appears to induce mitotic arrest by other mechanisms. To our knowledge, this is the first reported case where a time-dependent kinetic profiling approach has been utilized in a practical manner to a library of this size. The TCRP approach can also be extended to targets and pathways involved in other cellular processes.

## EXPERIMENTAL SECTION

**Cells.** HeLa, A549 and H1993 cells were obtained from ATCC. Cells were maintained in DMEM, F12K, and RPMI media respectively with 10% FBS and 1% penicillin and streptomycin. MCF7-ADR cell line is a kind gift from Dr. Fan in South Carolina Medical University. Cells were cultured in a 37 °C incubator with 5% CO<sub>2</sub>.

**Cell Index Calculation.** 2500–7000 cells were added to an E-Plate, a specialized microtiter plate used with the xCELLigence system (Roche). Cell attachment, spreading and proliferation were continuously monitored every 15–30 min using the xCELLigence system. The electronic readout, cell-sensor impedance, is displayed as an arbitrary unit called cell index (CI). CI at each time point is defined as (Rt-Rb)/15 where Rt is defined as the cell-electrode impedance of the well with the cells at different time points and Rb is defined as the background impedance of the well with the media alone. Normalized CI is calculated by dividing cell index at particular time points by the CI at the time of interest.

**siRNA Transfection, Drug Treatment, and Cell Proliferation Assays.** Silencer Select Validated siRNAs against PLK1 (PLK1-s450), KIF11 (KIF11-s7903 and KIF11-s7904) and control (CRTL2) siRNAs were purchased from Ambion. HP validated siRNAs against KIF11 (SI02653693, SI02653770, and SI03019793) were obtained from Qiagen. Mad2 siRNA was purchased from Dharmacacon. Reverse transfection with Lipofectamine RNAiMax was done following manufacturer's recommended procedure (Invitrogen). Briefly, desired amount of siRNA was mixed with lipid in 20 μL of Opti-MEM and incubated for 10 min in each individual well in 96-well E-Plates. Then, 2500–5000 cells in 100 μL media were added to the wells containing the siRNA-lipid mixture before the CI was monitored every 15–30 min using the xCELLigence system.

For compound treatment, 2500–7000 cells were seeded in the E-Plate. Twenty-four hours later, compounds were serially diluted and added to the culture. Cell-electrode impedance was then monitored using the xCELLigence system every 15–30 min to produce time-dependent cell response dynamic curves. Paclitaxel, vincristine, 5-FU, and dexamethasone were acquired from Sigma,

S-trityl-L-cysteine was purchased from Tocris, and staurosporine was obtained from CalBiochem.

**Gene Expression Analysis.** For RNA expression analysis of PLK1 and KIF11, HeLa cells were reverse transfected with 10 nM of the PLK1, KIF11 and the control siRNAs in either six-well plate ( $1.5 \times 10^5$  cells/well) or 96-well E-Plate (5000 cells/well). Total cellular RNA was obtained using High Pure RNA isolation kit (Roche) at time points of interests. Real-time RT-PCR was conducted using LightCycler 480 system (Roche). Gene specific primers and probes were designed using Universal Probelibrary assay design center, and purchased from IDTDNA and Roche, respectively. Real-time RT-PCR was conducted using the LightCycler 480 with the RNA Master Hydrolysis Probe mixture (Roche). Total cellular protein was made using RIPA buffer (Thermo Scientific) containing desired concentrations of complete protease inhibitors and phosphatase inhibitors (Roche). Mouse primary antibodies against KIF11 and GAPDH, and second antimouse HRP conjugated antibody were obtained from Santa Cruz Biotechnology. Results were scanned on an EpiChemII (UVP Bioimaging Systems), and mean pixel intensities in equivalent areas bounding each band were background corrected and quantified with ImageJ software (NIH). The extent of Eg5 protein knockdown was quantified by determining the ratio of the Eg5 to GAPDH band intensities for each treatment; % knockdown was calculated as the ratio of the resulting value for the Eg5 siRNA transfected lane to the control siRNA transfected lane.

**Mitotic Assays.** For immunofluorescence based mitotic index studies, transfected or compound treated cells grown on 16-well chamber slides (Lab-tec) were fixed in 100% ice-cold methanol at desired time point, washed in PBS, and permeabilized in PBS with 0.25% Triton X-100. Cells were then blocked with PBS containing 1% BSA and 0.1% TX-100. After washing with PBS, cells were stained with an antiphospho-Histone H3 (p-H3) antibody (S-10) (Millipore) and Rhodamine conjugated second antibody (Chemicon), followed by FITC-conjugated anti-α-tubulin antibody (Sigma) and antifade-DAPI (4',6-diamidino-2-phenylindole) (Invitrogen). Visualization and imaging was done using a Nikon E400 epifluorescence microscope and Nikon ACT software. Mitotic index was calculated by dividing the total number of p-H3 containing cells by the total number of DAPI stained cells. For each sample, cells from three different views were counted (30–80 cells/view) and mitotic index was calculated for each view, and average and standard deviation were shown.

For Elisa based mitotic assay studies, the colorimetric mitotic assay kits were used following manufacturer recommendations (Active Motif). Briefly, A549 cells were treated with compounds at 10 μM final concentration. Twenty hours after compound addition, when the CI was at the lowest value for paclitaxel treated cells, cells were fixed, stained with antiphospho-Histone H3 antibody, followed by HRP-conjugated secondary antibody. Colorimetric reaction was then carried out, and absorbance at OD<sub>450</sub> was determined using plate-reader (BTX 880, Beckman). Absorbance (Ab) values between 0.10 and 0.12 were consistently obtained for the control untreated cells, and compounds were classified based on their absorbance readings: +++ (Ab > 0.25); ++ (Ab, 0.20 – 0.25); + (0.15 – 0.20); - (<0.15).

(11) Abassi, Y. A.; Xi, B.; Zhang, W.; Ye, P.; Kirstein, S. L.; Gaylord, M. R.; Feinstein, S. C.; Wang, X.; Xu, X. *Chem. Biol.* **2009**, *16*, 712–723.

**Compound Library Screen.** A total of 119 595 compounds were obtained from ChemDiv. The primary screen was performed in H1993 at a single dose of 17.8  $\mu\text{M}$  using xCELLigence system for 48 h. We selected and confirmed 1149 hits in H1993 based on the criteria of 25% changes in CI relative to control at any time point post compound addition. These 1149 hits were then evaluated in A549 lung cancer cells using three different doses (17.8, 8.9, and 1.8  $\mu\text{M}$ ) to derive IC<sub>50</sub> values. Compounds with estimated IC<sub>50</sub> < 8.9  $\mu\text{M}$  were picked for clustering analysis as described<sup>11</sup> to identify antimitotic hits. Clustering analysis was done by calculating the distance among normalized CI curves for the first 24 h post compound addition. The antimitotic cluster was identified using paclitaxel as reference compound and visual inspection of the TCRP curves. A majority of the compounds in the antimitotic cluster were subject to p-Histone H3 based Elisa and/or immune-fluorescence assays in A549 cells. Sixteen most potent hits (with 1.8  $\mu\text{M}$  compound resulting in >50% CI changes compared to control) were chosen for multiple dose analysis in HeLa and MCF-7/ADR cells, and mitotic arrest was determined using mitotic index calculation.

**Tubulin Polymerization Assay.** Tubulin polymerization assay was conducted following manufacturer recommendation (Cytoskeleton). Briefly, 2 mg/mL tubulin (Cytoskeleton) was mixed with compounds of interests (15  $\mu\text{M}$  as final concentration), in the presence of 20% glycerol, 80 mmol/LPIPES, 2.0 mmol/L MgCl<sub>2</sub>, 0.5 mmol/L EGTA, pH6.9, and 1 mmol/L GTP. Paclitaxel (3  $\mu\text{M}$ ), vincristine (1.5  $\mu\text{M}$ ), or DMSO were applied in the assay as depolymerization, polymerization inhibitor and vehicle controls. The polymerization reaction was carried out and monitored at 37 °C every minute for at least 30 min in a plate reader (BTX 880, Beckman), with excitation and emission of 360 and 420 nm respectively.

## RESULTS

**Time-Dependent Cellular Response Profiles of Antimitotic Compounds.** We have previously demonstrated that impedance-based monitoring of cellular responses to biologically active small molecule compounds produces time-dependent cellular response profiles (TCRP), which can be predictive of mechanism of action of small molecule compounds.<sup>11</sup> Figure 1A shows the TCRP of HeLa cells that have been treated with small molecule compounds with different mechanisms including proteasome inhibitor (MG-132), tubulin-targeting drug (paclitaxel), DNA-damaging agent (5-FU), and nuclear steroid hormone agonist (dexamethasone). Each compound produced very specific TCRP that is modulated as a function of time and can be differentiated using the kinetic aspects of the impedance measurements. Importantly, compounds with similar mechanism of action produced very similar TCRP.<sup>11</sup> For example, well-known antimitotic compounds such as paclitaxel and vincristine produced dose-dependent signature antimitotic TCRP. This prototypical pattern consists of a time-dependent decrease in CI reaching a minimum point within 14 h after treatment (for HeLa cells) and followed by recovery of the CI. It is important to note that the extent of the time-dependent decrease in CI is cell type and concentration-dependent (Figure 1B). To better understand the cell biological and morphological changes that lead to the unique antimitotic TCRP, HeLa cells were treated with paclitaxel (33 nM) for different periods of time followed by fixation and staining of the cells with antitubulin antibody to monitor the

microtubule network and overall cell morphology (Figure 1E), phosphohistone H3 (p-H3) antibody to monitor cells undergoing or arrested at mitosis (Figure 1F),<sup>12,13</sup> and DAPI to stain nuclear DNA of cells (data not shown). Concurrently, parallel experiment was also set up in the E-Plate to monitor the CI changes (Figure 1C). As shown in Figure 1E and 1F, control cells at 0 h display a flattened morphology with well organized microtubule cytoskeleton and very few cells undergoing mitosis as evidenced by minimal number of cells stained by p-H3 antibody. In contrast, paclitaxel treated cells display enhanced p-H3 staining that is time-dependent; they begin to display rounded cell morphologies with intense staining of the polar microtubules, and increased staining of cells by p-H3 antibody by 7 h after compound treatment. By 14 h post compound addition, corresponding to the lowest point of the TCRP, more than 50% of cells display enhanced mitotic arrest phenotype as evidenced by rounded cell morphology and intense tubulin and p-H3 staining. Interestingly, by 24 and 38 h post compound addition, a large fraction of the cells appear to lose p-H3 staining and respread with irregular morphologies. To quantify the fraction of cells undergoing mitotic arrest, the mitotic index was calculated during different phases by dividing the number of p-H3 positive cells by total cell numbers recorded by DAPI staining. As shown in Figure 1C, mitotic index has an inverse relationship to the CI at the corresponding time points. Our observations are consistent with previous reports demonstrating that treatment of cells with tubulin targeting agents first leads to mitotic arrest, followed by mitotic slippage or mitotic escape and suggest that the unique antimitotic TCRP pattern recapitulates this phenomenon.<sup>7,14,15</sup>

**Validation of the Antimitotic TCRP.** Mitosis is a precisely choreographed set of events involving the participation of a plethora of proteins with diverse functions.<sup>7,10</sup> Interference with the function or expression of many of these proteins could lead to activation of the mitotic checkpoint and ultimately induction of mitotic arrest.<sup>5,7,8,10</sup> To further confirm the unique antimitotic TCRP pattern is indicative of mitotic arrest, we undertook a multipronged approach by studying cellular response to small molecule compound and siRNA-mediated modulation of specific targets involved in mitosis. We focused on mitotic kinesin motor protein Eg5, as both small molecule compounds and well validated siRNAs are available against this target.<sup>16,17</sup> Eg5 is a motor protein which plays a critical role during mitosis in the alignment and separation of sister chromatids, and interference in its expression or function by both siRNA and small molecule results in mitotic arrest.<sup>16–19</sup> HeLa cells were seeded in the E-Plate and treated with S-trityl-L-cysteine (STLC), a well-known inhibitor of Eg5 motor activity.<sup>16,17</sup> STLC treatment of HeLa cells resulted in TCRP very

- (12) Hendzel, M. J.; Wei, Y.; Mancini, M. A.; Van Hooser, A.; Ranalli, T.; Brinkley, B. R.; Bazett-Jones, D. P.; Allis, C. D. *Chromosoma* **1997**, *106*, 348–360.
- (13) Juan, G.; Traganos, F.; James, W. M.; Ray, J. M.; Roberge, M.; Sauve, D. M.; Anderson, H.; Darzynkiewicz, Z. *Cytometry* **1998**, *32*, 71–77.
- (14) Shi, J.; Orth, J. D.; Mitchison, T. *Cancer Res.* **2008**, *68*, 3269–3276.
- (15) Tao, W.; South, V. J.; Zhang, Y.; Davide, J. P.; Farrell, L.; Kohl, N. E.; Sepp-Lorenzino, L.; Lobell, R. B. *Cancer Cell* **2005**, *8*, 49–59.
- (16) DeBonis, S.; Skoufias, D. A.; Lebeau, L.; Lopez, R.; Robin, G.; Margolis, R. L.; Wade, R. H.; Kozielski, F. *Mol Cancer Ther.* **2004**, *3*, 1079–1090.
- (17) Skoufias, D. A.; DeBonis, S.; Saoudi, Y.; Lebeau, L.; Crevel, I.; Cross, R.; Wade, R. H.; Hackney, D.; Kozielski, F. *J. Biol. Chem.* **2006**, *281*, 17559–17569.
- (18) Weil, D.; Garcon, L.; Harper, M.; Dumenil, D.; Dautry, F.; Kress, M. *Biotechniques* **2002**, *33*, 1244–1248.
- (19) Zhu, C.; Zhao, J.; Bibikova, M.; Leverson, J. D.; Bossy-Wetzel, E.; Fan, J. B.; Abraham, R. T.; Jiang, W. *Mol. Biol. Cell* **2005**, *16*, 3187–3199.

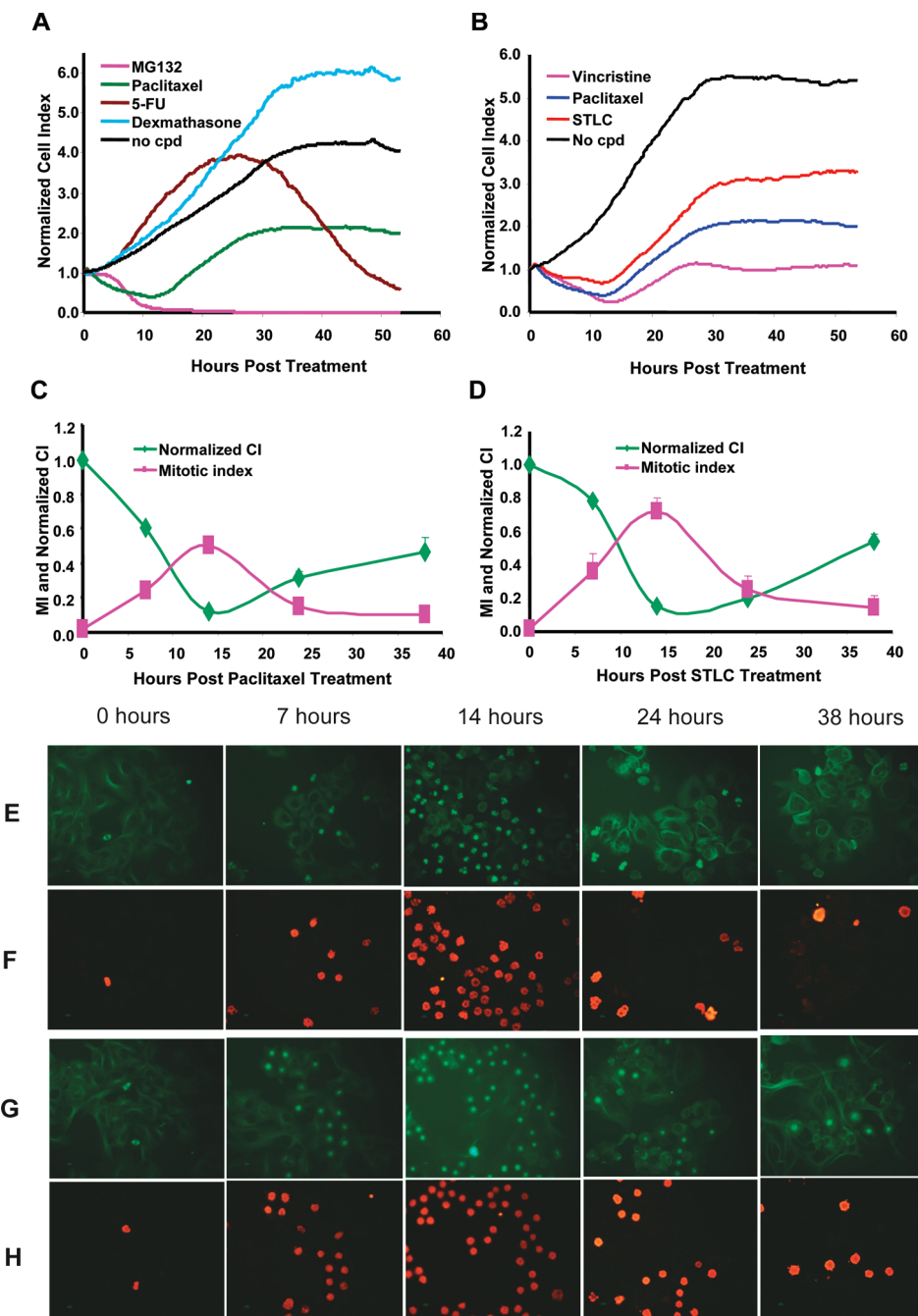


**Figure 1.** Time-dependent cellular response profiles mediated by antimitotic compounds. (A) HeLa cells cultured in E-Plates overnight were treated with MG-132 (10  $\mu$ M), paclitaxel (3.7 nM), 5-FU (11  $\mu$ M) and dexamethasone (100 nM). Cell index were continuously monitored for 54 h and normalized against the cell index at the time of treatment (time 0). Cells without compound treatment were used as control. (B) HeLa cells were treated with vincristine (0.41 nM), paclitaxel (3.7 nM) and S-trityl-L-cysteine (620 nM). Cell index were continuously monitored for 54 h and normalized against the cell index at the time of treatment. Cells without compound treatment were used as control. (C and D) HeLa cells cultured in E-Plate were treated with 33.3 nM paclitaxel (C) or 5.6  $\mu$ M S-trityl-L-cysteine (D). CI were continuously monitored for 54 h. Parallel experiments were also set up in Chamber slides to determine mitotic index at 0, 7, 14, 22, and 38 h post treatment. CI was normalized with the CI at the compound treatment and average of three individual wells was shown at the respective time points (0, 7, 14, 24, and 38 h post treatment). For mitotic index, 3–4 different fields (30–100 cells/view) under the fluorescence microscope were selected and mitotic index was derived by dividing the number of p-H3 positive cells with total cell numbers stained by DAPI. Average was shown and error bar indicates standard deviation. MI, mitotic index; CI, cell index. (E–H) Representative pictures were shown for paclitaxel treated cells stained with  $\alpha$ -tubulin (E) and p-H3 (F) and S-trityl-L-cysteine treated cells (G and H). Pictures of treated cells at different time points (0, 7, 14, 24, and 38 h post treatment) were shown.

similar to paclitaxel and vincristine, suggesting that the unique TCRP pattern is indeed indicative of mitotic arrest (Figure 1B). To confirm the correlation between STLC mediated TCRP with mitotic arrest phenotype, HeLa cells seeded in chamber slides were treated with STLC and the cells were fixed and stained with

p-H3 antibody, antitubulin antibody and DAPI as described for paclitaxel. Indeed, the time course of HeLa cell mitotic arrest mirrored that of paclitaxel (Figure 1D, G, and 1H).

Separately, HeLa cells were also transfected with various concentrations of KIF11 (the gene encoding Eg5) siRNA and

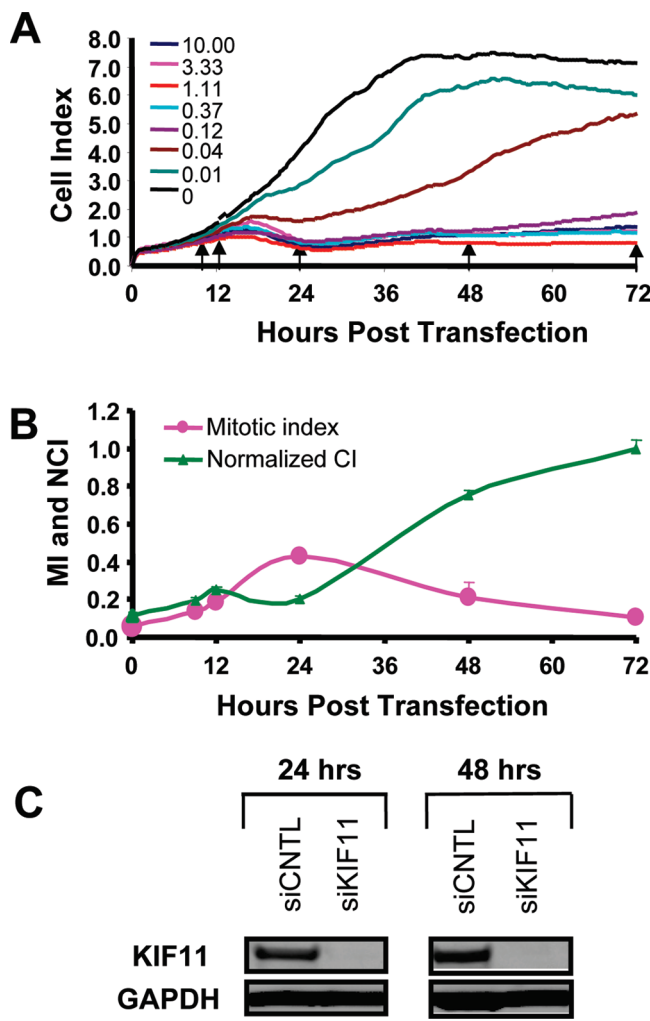


**Figure 2.** Time-dependent cellular response profiles mediated by KIF11 siRNA. (A) 3-fold serial diluted KIF11-s7904 siRNA (starting concentration 10 nM) were reverse transfected into HeLa cells and cell index was continuously monitored for 72 h. Arrows indicate time points when cell index and mitotic index were determined in B. (B) 10 nM KIF11-s7904 siRNA were used to transfected HeLa cells in E-Plate and chamber slide. Cell index was monitored in E-Plate continuously. CI at respective time points were normalized against cell index at 72 h to derive normalized cell index. Cells in chamber slides were stained with desirable markers to calculate mitotic index at different time points. Average of triplicate samples was shown and error bar indicates standard deviation. (C) HeLa cells were transfected with either control siRNA (siCNTL) or KIF11 siRNA (siKIF11-s7904). Total protein lysates were made 24 and 48 h post transfection. Western blot analysis was used to determine the KIF11 protein level. GAPDH was used as internal control.

cellular responses were continuously monitored (Figure 2A). A clear time and concentration-dependent antimitotic TCRP similar to STLC was observed, with higher siRNA concentrations producing more pronounced CI changes. The kinetics of the CI profiles is very similar between various concentrations of siRNAs: CI for the transfected samples started to diverge from the control samples starting 9–12 h post transfection, reaching the lowest level ~24 h post transfection, before starting to recover, indicating the specificity of the TCRP. However, siRNA mediated antimitotic TCRP is kinetically slower compared to compound mediated effect (Figure 1B), likely due to the slower kinetics of siRNA mediated target protein down-regulation.

To more precisely characterize siRNA mediated TCRP and its relationship to mitotic arrest phenotype, parallel experiments were set up in E-Plate to monitor CI changes, in chamber slides to determine mitotic index, and in 6-well plates to determine KIF11 mRNA and protein levels. Samples were taken at several time points post transfection (9 and 12 h when the siKIF11 transfected cells started to diverge from the siCNTL transfected cells; 24 h when the siKIF11 produced the strongest phenotype; 48 and 72 h when the CI started to increase), and subject to analysis. Down-regulation of KIF11 mRNA was observed as early as 9 h post transfection (88% down-regulation), continuing to 72 h, reaching 99% knockdown (data not shown). The KIF11 gene expression data is corroborated by analysis of Eg5 protein expression by Western blotting, achieving 97% and 100% knockdown at 24 and 48 h post transfection (Figure 2C). Down-regulation of KIF11 expression induces time-dependent mitotic arrest phenotype based on increased staining by anti-p-H3 antibody, and similar inverse relationship was observed between impedance based CI and mitotic index documented by the percentage of cells undergoing mitosis (Figure 2B). The continuous down-regulation of KIF11 mRNA and protein level indicates that the CI recovery phase observed at later time points is not due to loss of target down-regulation, and maybe explained by other reasons such as resprouting of the arrested cells due to mitotic escape. Similar siRNA mediated antimitotic TCRPs were also observed for four other KIF11 siRNAs (Supporting Information (SI) Figure 1A and B) and PLK1 (a serine/threonine protein kinase involved in cell cycle progression, especially in the formation of the mitotic spindle, and activation of CDKs/cyclins during mitosis)<sup>2,7,8</sup> siRNA (SI Figure 1C and D), while no or minimal response was seen for control siRNAs (data not shown), further validating the antimitotic TCRP.

In addition to the qualitative nature of the TCRP, CI can also predict siRNA functions quantitatively, as higher siRNA concentrations produced more pronounced CI changes (Figure 2A), correlating with target down-regulation (SI Figure 1E) and higher mitotic index (SI Figure 1F). Similar quantitative prediction of mitotic arrest by CI was also observed for antimitotic compounds, for example, paclitaxel (data not shown). In summary, our data clearly indicates that the unique antimitotic TCRP is a signature profile for cells undergoing mitotic arrest and eventually mitotic escape.

**Dependence of Antimitotic TCRP on Spindle Assembly Checkpoint Machinery.** As mentioned previously, microtubule poisons as well as Eg5 inhibitors induce mitotic arrest by activating the spindle assembly checkpoint.<sup>5,7–9</sup> Down regulation of the protein components of the mitotic checkpoint such as Mad2, has been shown to result in insensitivity of treated cells to antimitotic agents such as paclitaxel.<sup>20,21</sup> We were therefore interested in determining if inhibition of the mitotic checkpoint through down regulation of Mad2 protein by siRNA, can lead to a loss of the antimitotic TCRP. HeLa cells first transfected either with a control siRNA or Mad2 siRNA were treated with paclitaxel, vincristine and STLC. While tubulin poisons and Eg5 inhibitor produced antimitotic TCRP in control siRNA transfected cells (Figure 3A), the antimitotic TCRP was significantly abolished in siMad2

(20) Chin, G. M.; Herbst, R. *Mol. Cancer Ther.* 2006, 5, 2580–2591.

(21) Sudo, T.; Nitta, M.; Saya, H.; Ueno, N. T. *Cancer Res.* 2004, 64, 2502–2508.

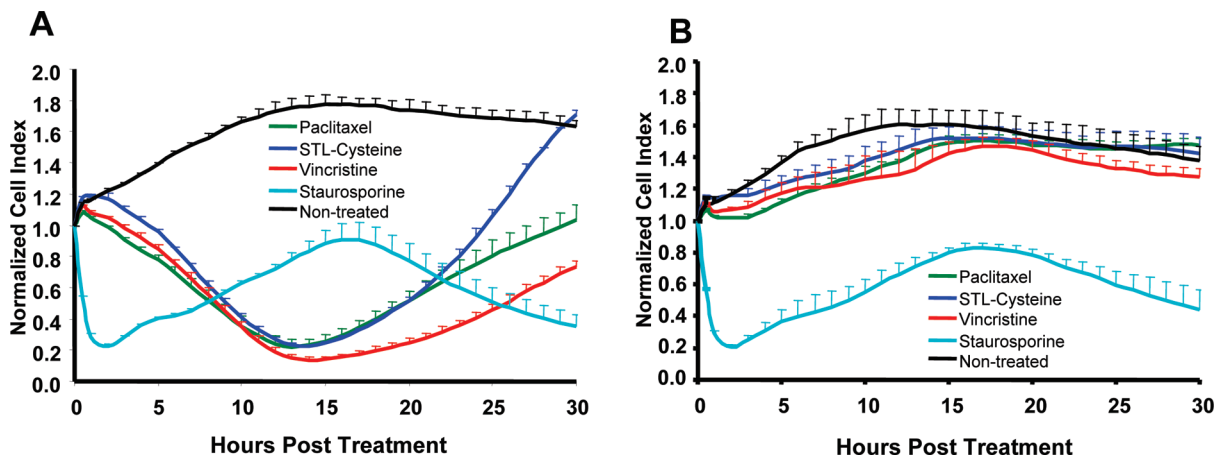


**Figure 3.** Dependence of antimitotic TCRP on spindle checkpoint machinery. HeLa cells were transfected with either control siRNA (A) or Mad2 siRNA (B) and seeded in E-Plates. Twenty-four hours later, cells were treated with paclitaxel (33 nM), S-trityl-L-cysteine (1.8  $\mu$ M), vincristine (3.7 nM) and staurosporine (110 nM). Nontreated samples were used as control. Cell index was monitored continuously for 30 h and normalized against the cell index at time of compound addition. Average of triplicate samples was shown. Error bar indicates standard deviation.

transfected cells (Figure 3B). In contrast, minimal TCRP difference was observed between the control or Mad2 siRNA transfected cells when treated with a control compound, staurosporine, which does not cause mitotic arrest (Figure 3A and B). Therefore, the antimitotic TCRP is dependent on the intact spindle assembly checkpoint machinery, again establishing the specificity of this unique pattern.

**Impedance-Based Cytological Profiling As a Screening Tool to Identify Compounds That Induce Mitotic Arrest.** Using molecular and cellular assays, we have thus far demonstrated and validated the antimitotic TCRP mediated by both small molecule compounds and siRNA mediated target down-regulation. While a number of compound profiling strategies including high content screening, gene expression profiling, cytotoxicity-based profiling and proteomic profiling have been reported in the literature, the majority of these profiling approaches have been performed with limited number of compounds at a single time-point and mainly for proof of principle studies.<sup>22–24</sup> We wanted to explore the practicality and predictivity of the TCRP-based screening approach using a large compound library to determine if we can identify and characterize novel antimitotic compounds. We acquired 119595 compounds library from ChemDiv and conducted the screen using xCELLigence RTCA system which allows for measurement of compound-mediated TCRP. The library was screened at a final concentration of 17.8  $\mu$ M using H1993 cells growing in the E-Plate. A total of 1149 hit compounds with several TCRP of interests were identified and confirmed in H1993 cells (Figure 4A). Multidose confirmation studies were conducted in A549 cell line, and 239 hits with estimated IC<sub>50</sub> < 8.9  $\mu$ M were selected and their TCRPs were subject to clustering analysis to identify compounds which produced antimitotic TCRP. Out of 239 hits, 125 compounds' TCRPs coclustered with well-known antimitotic agents such as paclitaxel and were identified as potential

antimitotic hits (Figure 4B). A total of 117 compounds from the antimitotic cluster were further tested for their ability to mediate mitotic arrest using the phospho-Histone H3 based Elisa assay in A549 (109 compounds, SI Figure 2) and fluorescence based mitotic index assay in HeLa (16 compounds, Table 1). Interestingly, 113 of the 117 compounds in the TCRP cluster led to increased p-H3 staining (Figure 4B). Closer inspection of the four negative compounds in p-H3 Elisa assay revealed that their TCRPs did not closely match the typical mitotic arrest TCRP (SI Figure 2). In summary, the validation of mitotic hits indicates the robust predictive nature of the TCRP based clustering approach.

To determine whether these antimitotic compounds may offer advantages over current therapies, we focused on 16 potent antimitotic compounds (IC<sub>50</sub> < 1.8  $\mu$ M) and tested them in chemotherapy-resistant MCF7-ADR cell line (resistant to paclitaxel and adriamycin due to overexpression of MDR gene<sup>25</sup>). Significantly, all 16 compounds induced robust antimitotic TCRP in MCF7-ADR cell lines, with IC<sub>50</sub> similar to HeLa cells. This is in contrast to the >300 fold sensitivity difference observed for paclitaxel (Table 1). Furthermore, tubulin polymerization assay revealed that 12 of the 16 compounds target tubulin polymerization while the remaining four of the 16 compounds do not appear to have effect on tubulin polymerization at 15  $\mu$ M compound concentration (Table 1). Therefore, these compounds have the potential to be further pursued as novel antimitotic agents. Based on Pubchem search on these compounds, four have previously been reported as tubulin-targeting agents, four reported with cytotoxic effects with unknown mechanisms, while the other eight either have no reported activity or have not been tested before (Table 1).

It is also of interest that out of the 16 compounds, five share similar structures and are imidazo-pyrimidinyl/pyridinyl 2-amino thiazole derivatives. All five compounds induce the signature dose-dependent antimitotic TCRP with IC<sub>50</sub> between 9 and 44 nM and mitotic arrest phenotype was confirmed by mitotic index determination (Table 1, Figure 5). The antimitotic activity of these compounds is most likely due to inhibition of tubulin polymeri-

- (22) Perlman, Z. E.; Slack, M. D.; Feng, Y.; Mitchison, T. J.; Wu, L. F.; Altschuler, S. J. *Science* **2004**, *306*, 1194–1198.
- (23) Wagner, B. K.; Clemons, P. A. *Curr. Opin. Chem. Biol.* **2009**.
- (24) Feng, Y.; Mitchison, T. J.; Bender, A.; Young, D. W.; Tallarico, J. A. *Nat. Rev. Drug Discov.* **2009**, *8*, 567–578.

- (25) Fairchild, C. R.; Ivy, S. P.; Kao-Shan, C. S.; Whang-Peng, J.; Rosen, N.; Israel, M. A.; Melera, P. W.; Cowan, K. H.; Goldsmith, M. E. *Cancer Res.* **1987**, *47*, 5141–5148.

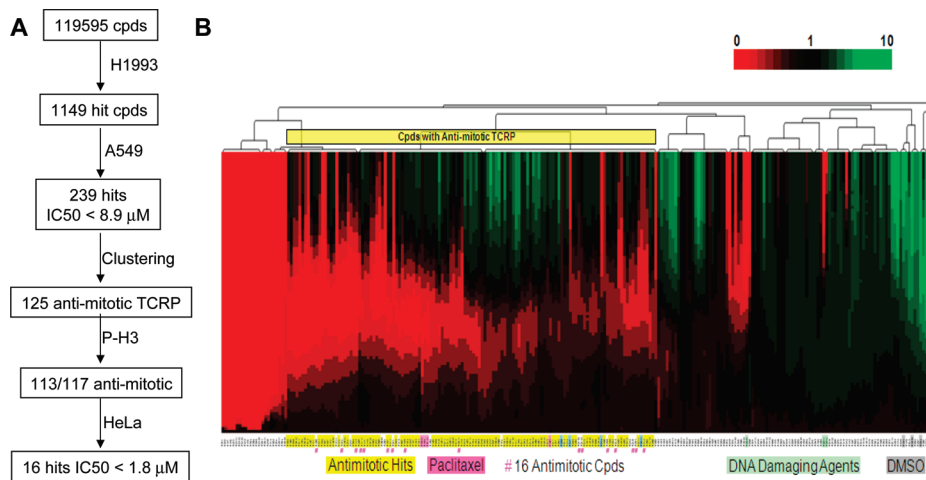


**Figure 4.** Antimitotic TCRP based compound screening. (A) Screening flowchart is shown. (B) Clustering analysis of hit compounds identified from the screen. Agglomerative, hierarchical clustering analysis of 239 hits identified was shown. The descriptor is the change in cell index as a function of time. X-axis indicates compound code and Y-axis indicates normalized cell index at different time points. TCRP of compounds at 17.8  $\mu$ M in A549 for the first 25 h post compound treatment was used for the clustering analysis. Paclitaxel (50 nM) from four different plates (highlighted in pink) was used as reference antimitotic compound. Camptothecin (80  $\mu$ M), doxorubicin (20  $\mu$ M), and methotrexate (20  $\mu$ M) were used as reference compounds for DNA-damaging agents (highlighted in green). DMSO controls from four different plates were highlighted in gray. 125 compounds with antimitotic TCRP were identified (yellow bar). 109 compounds were tested in p-H3 based Elisa assay and antimitotic compounds were highlighted in yellow and nonantimitotic compounds were highlighted in blue. Sixteen compounds were analyzed in mitotic index assay as shown in Table 1 and are indicated by “#” in pink.

**Table 1. Summary of Anti-Mitotic Compounds Identified through the Screen**

ACEA <sup>a</sup>	mitotic Index		IC50 (nM)			MTP	Pubchem
	average	std deviation	HeLa	MCF7-ADR	ratio		
ACEA100160	0.60	0.09	9.2	27	2.9	+	TI
ACEA100282	0.69	0.10	25.8	85.6	3.3	+	NA
ACEA100283	0.30	0.03	17.2	48.6	2.8	+	NA
ACEA100285	0.69	0.08	12.6	39.5	3.1	+	CT
ACEA100286	0.37	0.05	44.4	101.1	2.3	+	TI
ACEA100162	0.79	0.04	10.2	37.3	3.7	+	TI
ACEA100281	0.66	0.06	560.8	649.5	1.2	-	NT
ACEA100284	0.50	0.15	1644.2	3031.7	1.8	+	NT
ACEA100287	0.48	0.10	193.7	469.8	2.4	+	NT
ACEA100288	0.47	0.03	202.7	318.8	1.6	+	NA
ACEA100289	0.48	0.02	896.1	1485.3	1.7	+	CT
ACEA100290	0.48	0.06	89.6	125.9	1.4	-	NT
ACEA100291	0.51	0.07	200.6	401.8	2.0	+	TI
ACEA100292	0.54	0.10	639.9	1007.7	1.6	+	CT
ACEA100293	0.50	0.02	1682.1	2602.2	1.5	-	CT
ACEA100294	0.54	0.10	360.3	386.7	1.1	-	NT
paclitaxel	0.50	0.03	3.3	>1000	>300	+	
vincristine	0.69	0.03	0.5	>10	>20	+	
STL-cysteine	0.72	0.06	779.5	9763.2	12.5	-	
No cpd	0.03	0.02	N/A	N/A	N/A	N/A	

<sup>a</sup> Compound code is shown. For Mitotic index, HeLa cells were seeded in Chamber Slide and treated with desired concentrations of compounds (A160, 100 nM; A282, 370 nM; A283, 123 nM; A285, 370 nM; A286, 123 nM; A162, 100 nM; A281, 1.1  $\mu$ M; A284, 10  $\mu$ M; A287, 370 nM; A288, 370 nM; A289, 1.1  $\mu$ M; A290, 370 nM; A291, 370 nM; A292, 1.1  $\mu$ M; A293, 3.3  $\mu$ M; A294, 1.1  $\mu$ M; paclitaxel, 33.3 nM; vincristine 3.7 nM; STLC, 5.6  $\mu$ M) for 14–16 h before cells were fixed and stained. Calculation of mitotic index was described in Methods. For IC50 determination, HeLa and MCF7/ADR cells seeded in E-Plates were treated with various concentrations of each compound. IC50 was calculated using RTCA 1.2 software. Ratio was calculated by dividing the IC50 in MCF7-ADR by the IC50 in HeLa. For tubulin polymerization assay (MTP), assay was conducted per manufacturer recommendation. +, compound has effect on tubulin polymerization (>20% from control at 15  $\mu$ M); -, compound has no effect on tubulin polymerization (<20% from control at 15  $\mu$ M). For PubChem information, structural search was conducted. TI, tubulin interfering activity reported; CT, cytotoxicity activity reported; NA, no activity (or no cytotoxic activity) reported; NT, not tested.

zation (Table 1). Other compounds with similar structures have been reported previously as potent modulators of transcriptional repression in Huntington's disease<sup>26,27</sup> and cytotoxic agents.<sup>27</sup>

Collectively, these data reveal that TCRP can be used in a predictive manner to identify compounds that induce mitotic

arrest. These compounds can include novel tubulin targeting agents as well as compounds targeting other proteins the inhibition of which may induce mitotic arrest, and warrants further pursuit for novel antimitotic based therapies.

(26) Leone, S.; Mutti, C.; Kazantsev, A.; Sturlese, M.; Moro, S.; Cattaneo, E.; Rigamonti, D.; Contini, A. *Bioorg. Med. Chem.* **2008**, *16*, 5695–5703.

(27) Rigamonti, D.; Bolognini, D.; Mutti, C.; Zuccato, C.; Tartari, M.; Sola, F.; Valenza, M.; Kazantsev, A. G.; Cattaneo, E. *J. Biol. Chem.* **2007**, *282*, 24554–24562.

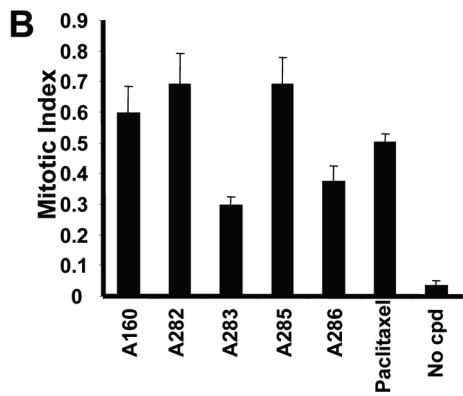
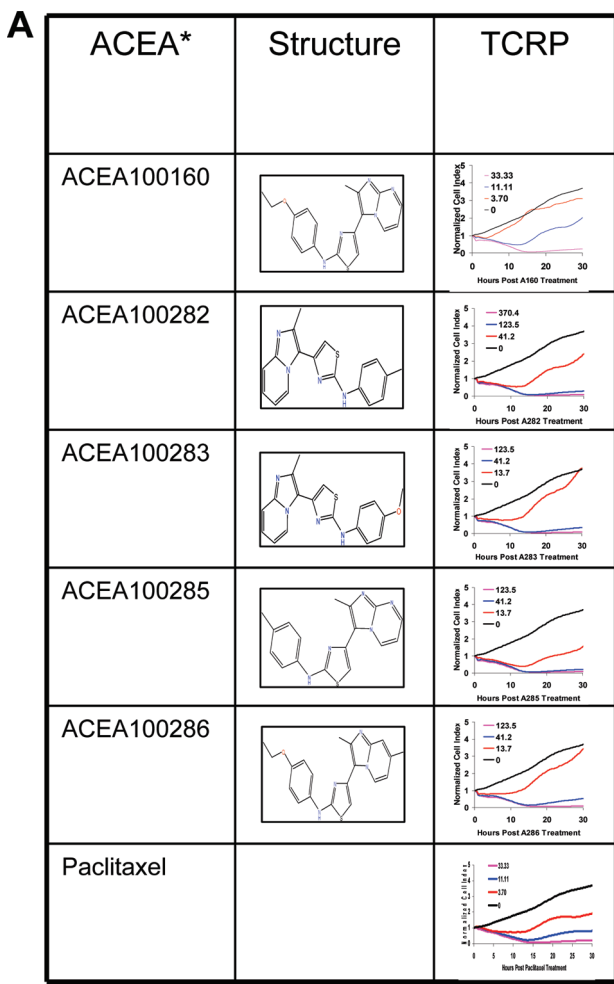


**Figure 5.** (A) Structures of ACEA100160 series compounds and their antimitotic patterns in HeLa were shown. (B) Mitotic index was determined in HeLa cells for A160 (100 nM), A282 (370 nM), A283 (123 nM), A285 (123 nM) and A286 (123 nM). Paclitaxel (33.3 nM) was used as positive control, and untreated samples were used as negative control.

## DISCUSSION

We have previously demonstrated that compounds with similar mechanism of actions produce similar impedance-based TCRP.<sup>11</sup> In this report, we have focused on and further characterized a reproducible and specific type of TCRP that is produced in response to antimitotic drugs and compounds. We have demonstrated that the impedance-based TCRP correlates with the induction of mitotic arrest and subsequent mitotic escape using

both small molecule and siRNA approaches. Furthermore, disabling the mitotic checkpoint through siRNA-mediated down-regulation of Mad-2 abolished the antimitotic TCRP induced by antimitotic compounds, indicating that this profile is indeed specific for induction of mitotic arrest. The qualitative and quantitative prediction of mitosis arrest by TCRP makes it possible to systematically examine compounds or targets' effects on mitotic machinery. In addition, it is also possible to use TCRP as a screening approach to identify novel compounds or targets involved in mitosis. We used the TCRP approach to screen a ~120 000 compound library and identified compounds that interfere with mitotic machinery based on clustering analysis. Out of the 117 potential antimitotic hits identified by clustering analysis, 113 were confirmed by independent assays, whereas none of the 10 compounds that were outside of the antimitotic cluster produce positive p-H3 staining (data not shown), indicating the robust predictive nature of TCRP based screening. Interestingly, the four compounds that were not confirmed did not display the signature antimitotic TCRP by visual inspection (SI Figure S2). This indicates that as with any clustering analysis, the TCRP based approach should be only used as guidance, and hit compounds should be confirmed by a combination of visual inspection of the TCRPs and experimental validation at multiple doses. In addition, the accuracy of prediction will also depend on the potency of the compounds as potent compounds more likely display the prototypical TCRP and can therefore be identified more accurately, as in the case of TCRPs mediated by different concentrations of paclitaxel (SI Figure S2). The importance of this novel antimitotic screening was shown by successful identification of nontubulin interfering agents and compounds that induced mitotic arrests in MCF7-ADR cell line that is resistant to a wide range of chemotherapeutic agents, including taxane and *vinca* alkaloid, due to overexpression of MDR protein.<sup>25</sup> Recent efforts have been directed at targeting the mitotic checkpoint and mitotic exit machineries in order to increase the clinical efficacy of antimitotic therapeutics, and the real-time monitoring of antimitotic TCRP would be a good tool in aiding to identify novel agents mediating these processes.<sup>28–32</sup>

Recently, the drug discovery process itself has been undergoing a certain degree of paradigm shift from biochemical-based screening to cell-based screening.<sup>24</sup> The main reason for this shift has been due to the fact that cell-based phenotypic assays are thought to more closely recapitulate the complexity of the whole living organism, and at the same time can be used to reveal unwanted side effects such as toxicity at the cellular level. However, cell-based screening is often not as specific as biochemical-based screening and is therefore often termed “black box” screens, as single target mediating the compound effect is rarely revealed.<sup>24</sup> As a compromise between assay complexity and specificity, multidimensional profiling approaches including gene-

- (28) DeMoe, J. H.; Santaguida, S.; Daum, J. R.; Musacchio, A.; Gorbsky, G. J. *Cancer Res.* **2009**, *69*, 1509–1516.
- (29) Huang, H. C.; Shi, J.; Orth, J. D.; Mitchison, T. J. *Cancer Cell* **2009**, *16*, 347–358.
- (30) Riffell, J. L.; Zimmerman, C.; Khong, A.; McHardy, L. M.; Roberge, M. *Cell Cycle* **2009**, *8*, 3025–3038.
- (31) Salmela, A. L.; Pouwels, J.; Varis, A.; Kukkonen, A. M.; Toivonen, P.; Halonen, P. K.; Perala, M.; Kallioniemi, O.; Gorbsky, G. J.; Kallio, M. J. *Carcinogenesis* **2009**, *30*, 1032–1040.
- (32) Stolz, A.; Vogel, C.; Schneider, V.; Erych, N.; Kienitz, A.; Yu, H.; Bastians, H. *Cancer Res.* **2009**, *69*, 3874–3883.

expression based profiling, proteomic-based profiling, multipathway based profiling have been proposed to understand the complexity of compound action and to generate hypothesis as to the potential mechanism of action of the compounds of interest.<sup>22–24</sup> To capture information regarding the specificity of a compound for certain targets and pathways in these approaches, sophisticated bioinformatics softwares are utilized to search for patterns or signatures of activity specific for particular pathways or cellular processes.

One of the main obstacles for wider adoption of these techniques for actual primary screening has been the fact that these techniques are highly resource intensive and requires very sophisticated bioinformatics tools to capture meaningful information. Therefore, these approaches have mainly been used on small subset of compounds and mainly for proof of principle studies rather than as a practical tool that can be readily implemented in the drug discovery process. The other drawback is that most if not all multidimensional profiling approaches are performed at one single time points, and it is likely that interesting compound activities may be missed.<sup>33</sup> The TCRP approach discussed in this work and elsewhere<sup>11</sup> provides several unique advantages. First, it is a kinetic-based assay and therefore the profiles can reveal information about the time-dependent compound effect (both desirable on-target effect and undesirable off-target effect) which can be missed by other profiling approaches. Second, the profiles generated are a reflection of the inherent global cellular response to a specific treatment, without having to artificially engineer the cell with any reporter proteins. Once validated, the signature profiles can provide very specific information about cellular pathways being modulated. Third, the TCRP are quantitative; as we have shown here for both compound and siRNA modulation of the antimitotic TCRP. The extent of CI changes is directly proportional to the amount of siRNA being transfected or to the concentration of compound added to the cell. Finally, this profiling procedure is practical for actual screening of compound libraries allowing for identification of novel compounds modulating mitosis.

In addition to the impedance-based antimitotic TCRP described here, we have observed other distinct profiles, for example, DNA damaging, cytostatic, and glucocorticoids.<sup>11</sup> The present study

(33) Neumann, B.; Held, M.; Liebel, U.; Erfle, H.; Rogers, P.; Pepperkok, R.; Ellenberg, J. *Nat. Methods* 2006, 3, 385–390.

suggests that by expanding the biological space at which a compound is being screened and introducing time resolution into the assay provides unique profiles which can be used to categorize compounds with important biological activities based on their mechanism of action. This approach is information intensive with time-resolved cellular responses and can be used to complement other screening or profiling approaches.

## CONCLUSIONS

Cell-based screening is increasingly utilized in the drug discovery and development field. One of the main hurdles to wider adoption of cell-based assays has been that cell-based assays are often not as specific as biochemical assays. Multidimensional cell-based profiling approaches have been proposed as a way to overcome the “black box” phenomenon of cell-based assays and help reveal mechanism of compound action. Perturbation of biological functions is associated with very precise changes in cell proliferation, cell morphology, and cell adhesion, which could be indicative of mechanism of compound action. Using the time resolution of impedance technology we have characterized a specific time-dependent cellular profile (TCRP) for compounds inducing mitotic arrest. The specificity of the mitotic arrest TCRP was confirmed using both RNAi and small molecule approaches. We used the TCRP approach to screen a 120 000 compound library and identified novel small molecule compounds which perturb mitosis. Thus, our work demonstrates the feasibility of using TCRP approach for both target identification and for screening of small molecule compounds which specifically perturb mitosis.

## ACKNOWLEDGMENT

The authors are employed by ACEA Biosciences, which is manufacturer of the xCELLigence system utilized in this work.

## SUPPORTING INFORMATION AVAILABLE

SI Figures 1 and 2 and an anti-mitotic cluster chart. This material is available free of charge via the Internet at <http://pubs.acs.org>.

Received for review March 26, 2010. Accepted June 1, 2010.

AC1007877